Sensor and Simulation Notes

Note 560

5 June 2012

A NEW SET OF ELECTRODES FOR COAXIAL, QUARTER WAVE, SWITCHED OSCILLATORS

Felix Vega

EMC Laboratory, Swiss Institute of Technology of Lausanne, EPFL, Switzerland

National University of Colombia, Bogota, Colombia

Farhad Rachidi

EMC Laboratory, Swiss Institute of Technology of Lausanne, EPFL, Switzerland

D.V. Giri

Dept. of ECE, University of New Mexico, Albuquerque
Pro-Tech, 11-C Orchard Court, Alamo, CA

Abstract - We present a new profile for the electrodes forming the radial transmission line of a switched oscillator (SWO). The profile is formed using a curvilinear orthogonal space, based on a specific 2-D transformation called Logarithmic-Tangent (Ln-Tan). The proposed profile results in an optimal distribution of the electric field, with a peak amplitude occurring on the axis of symmetry of the SWO, and a smooth, monotonic decrease in amplitude, as we move away from the discharge point towards the coaxial transmission line. Moreover, the proposed profile assures a smooth continuity (up to the first space derivative) at the junction of the RTL-coaxial line. Numerical simulation results on the electric field distribution in the SWO are presented and discussed.

1. INTRODUCTION

A Switched Oscillator (SWO) is a mesoband radiating system proposed by Baum in [1]. The system consists of a DC-charged low-impedance coaxial transmission line that is discharged at one end by a spark gap and is connected at the other end to a high impedance antenna. During the charging phase, the capacitor formed by the SWO is slowly charged until breakdown occurs at the pressurized spark gap end. The wave produced propagates towards the antenna. Due to the mismatch between the coaxial transmission line and the antenna, only part of the energy is radiated; Most of the energy is reflected back to the spark gap, where the wave is re-reflected by the low-impedance arc. The reflections occurring at this point, opposite in sign, produce a damped sinusoid-like signal with a central frequency of about $f=v_p/4L$, where L is the length of the line and v_p is the wave propagation velocity.

The overall geometry of an SWO is depicted in Figure 1. Notice that the electrodes of the spark gap form a radial transmission line (RTL) that progressively become a low-impedance coaxial transmission line which is further connected to the antenna.

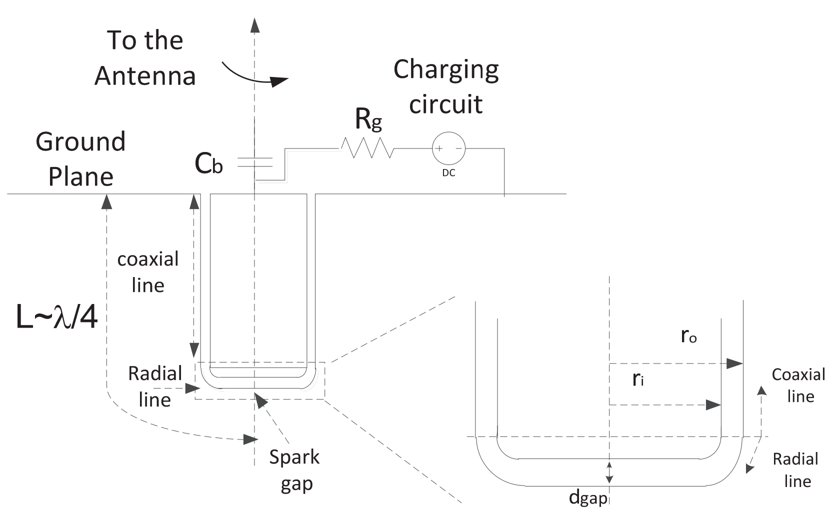

Figure 1 Quarter wave coaxial switched oscillator (SWO). Notice the presence of the RTL at the low impedance end of the SWO. Any type of antenna can be connected to the SWO.

The electrostatic field distribution of the structure (prior to the discharge) should guarantee the occurrence of a fast discharge between the electrodes, on the symmetry axis of the SWO. Therefore, the geometry must maximize the electric field at the discharge point and prevent field enhancements or distortions that could lead to the occurrence of discharges in other points of the geometry.

We propose in this paper a new profile for the electrodes forming the RTL of an SWO. The profile is formed using a curvilinear orthogonal space, generated from a 2-D transformation, called Logarithmic-Tangent (Ln-Tan), proposed by Moon and Spencer in [2] (page 67). The advantage of this profile is that it assures that the maximum amplitude of the electric field occurs on the axis of symmetry, while the field intensity decreases as we move away from the discharge point towards the coaxial transmission line. More importantly, the proposed profile assures a smooth continuity (up to the first space derivative) at the junction of the RTL-coaxial line.

2. BACKGROUND

Assuming isotropic and time invariant conditions, the electrostatic field distribution between the electrodes of a gas spark gap depends mainly on the shape of the metallic surface of the electrodes. The occurrence of dielectric breakdown depends on many factors such as gas density, distance between electrodes, electric field intensity and roughness of the metallic surface. The choice on the profile of the electrodes permits, for example, to control the occurrence of field enhancements in specific regions.

The design of electrodes for spark gaps used in applications such as Marx generators and Ultra Wide Band (UWB) pulsers rely mostly on the profiles proposed by Rogowski[3], Ernst[4] and Bruce[5], which are intended to produce a uniform field distribution in a defined volume of the inter-electrodic space. These profiles improve the repeatability of the discharge and distribute the point of origin of the arc homogeneously on the surface of the electrodes, assuring a uniform wearing of the metallic surface. In general, in such applications the size of the electrodes is much smaller than the smallest wavelength of the discharge pulse; therefore, propagation effects can be neglected.

In the case of an SWO, the situation is quite different. In order to prevent distortion of the signal transmitted to the antenna, the discharge should be produced exactly on the axis of symmetry of the SWO so that all the points on the wavefront originated at the discharge point would get simultaneously to the antenna.

The problem of the distribution of the electrostatic field in an SWO has been discussed by Giri *et al.* in [6]. A more detailed discussion and design technique was proposed by Armanious *et. al,* in [7], where the profile of the RTL varies linearly towards the coaxial. The transition or bend between the RTL and the coaxial is designed using an iterative method, based on the equivalent charge distribution principle. The formed geometry produces an electric field that is maximum on the axis of symmetry and decreases as one moves towards the coaxial. However, the electric field exhibits an undershoot in the bend region. This can be reduced by increasing the number of iterations, but, by doing so, the rate of decreasing of the electric field is also changed.

We propose in the next section a new set of electrodes that maximizes the electric field on the axis and additionally generates a field distribution that smoothly and monotonically decreases as we move away from the axis.

3. CONDITIONS FOR OPTIMAL ELECTROSTATIC DISTRIBUTION

The probability of producing breakdown on the axis of symmetry maximizes if the magnitude of the electrostatic field at the time of occurrence of the discharge is maximum at the axis of symmetry of the SWO, between the electrodes. The conditions necessary to produce the desired field distribution are

i) The distance between the electrodes should be minimum at the axis of symmetry.
ii) The distance between the electrodes should monotonically increase as we move towards the coaxial line.
iii) The profile of the electrodes as well as its first space derivative should be continuous.

On the other hand, the inter-electrodic distance at the axis d_{gap} and the cross sectional dimensions of the coaxial transmission line r_{in}, r_{out} (as defined in Fig. 1) are generally specified parameters and can be included in the analysis as two additional conditions:

iv) The distance between the electrodes at the axis of symmetry should be d_{gap}.

v) At the junction point between the electrodes and the coaxial transmission line, the profile of the electrodes should coincide with the dimensions of the coaxial transmission line. r_o, r_i,

A set of curves fulfilling these conditions can be formed using an orthogonal curvilinear space, based on the conformal Ln-Tan transformation proposed by Moon and Spencer in [2].

4. A METHOD FOR GENERATING A CURVILINEAR COORDINATE SPACE FROM CONFORMAL TRANSFORMATIONS

The method of generating a curvilinear space starting from a conformal transformation was proposed by Moon and Spencer in [8]. The method consists basically of performing a conformal transformation from the *W* to the Z plane. The orthogonal curved lines produced on the *Z* plane can be regarded as a 2-D curvilinear coordinate system, which can be either translated or rotated, in order to generate a 3-D coordinate system. The procedure can be summarized as follows:

The transformation from the W to Z complex planes is;

$$Z = f(W) \tag{1}$$

where:

f is an analytical function; *W* and *Z* are complex planes:

$$\begin{aligned} W &= u + iv \\ Z &= x + iy \end{aligned} \tag{2}$$

As the angles are preserved by the transformation, the function *f* maps the rectangular grid defined by the lines *u=const* and *v=const* in the *W* plane, into an orthogonal curvilinear grid in the *Z* plane.

The parametric form of this new set of orthogonal curves can be obtained from the real and imaginary parts of Equation (1) as:

$$\begin{aligned} x &= f_1(u,v) = \mathrm{Re}[f(W)] \\ y &= f_2(u,v) = \mathrm{Im}[f(W)] \end{aligned} \tag{3}$$

The resulting curvilinear grid can be used to generate new coordinate systems. For example, if the *Z* plane is extruded in a perpendicular direction, a cylindrical coordinate system *(u, v, w)*can be obtained, where the relationship with the Cartesian coordinates is:

$$\begin{aligned} x &= f_1(u,v) \\ y &= f_2(u,v) \\ z &= w \end{aligned} \tag{4}$$

If, on the other hand, the *Z* map is rotated around the original *y* axis, we obtain a rotational coordinate system *(u v, w).* The new relationships with the Cartesian coordinates are given by:

$$\begin{aligned} x &= f_1(u,v)Cos(w) \\ y &= f_1(u,v)Sin(w) \\ z &= f_2(u,v) \end{aligned} \tag{5}$$

A similar procedure can be applied if the map is rotated around the *x* axis.

In this new coordinate system, the infinitesimal arc length element *(dl)* can be calculated as [2]:

$$dl^2 = \sqrt{g_{11}du^2 + g_{22}dv^2 + g_{33}dw^2} \tag{6}$$

where the metric coefficients g_{ii} are defined as:

$$
\begin{aligned}
g_{11} &= \left(\frac{\partial x}{\partial u}\right)^2 + \left(\frac{\partial y}{\partial u}\right)^2 + \left(\frac{\partial z}{\partial u}\right)^2 \\
g_{22} &= \left(\frac{\partial x}{\partial v}\right)^2 + \left(\frac{\partial y}{\partial v}\right)^2 + \left(\frac{\partial z}{\partial v}\right)^2 \\
g_{33} &= \left(\frac{\partial x}{\partial w}\right)^2 + \left(\frac{\partial y}{\partial w}\right)^2 + \left(\frac{\partial z}{\partial w}\right)^2
\end{aligned} \tag{7}
$$

The metric coefficients permit, for example, to calculate the infinitesimal arc lengths along a coordinate axes *u, v or w*:

$$
\begin{aligned}
dl_u &= \sqrt{g_{11}}\,du \\
dl_v &= \sqrt{g_{22}}\,dv \\
dl_w &= \sqrt{g_{33}}\,dw
\end{aligned} \tag{8}
$$

5. THE LOGARITHMIC TANGENT (Log-Tan) COORDINATE SYSTEM

The conformal transformation, generating the Log - Tan coordinate system is:

$$
Z = \frac{2a}{\pi} \ln\left(\tan\left(W\right)\right) - ia \tag{9}
$$

where:

$$
\begin{aligned}
W &= u + iv \\
Z &= x' + iy'
\end{aligned} \tag{10}
$$

u and *v* are defined in the domain:

$$
\begin{aligned}
&0 \le u < \pi / 2 \\
&0 \le v
\end{aligned} \tag{11}
$$

While *x', y'* are defined in:

$$
\begin{aligned}
&-a \le y' \le a \\
&-\infty < x' < \infty
\end{aligned} \tag{12}
$$

Where *a* > 0 is a constant.

Notice that the apostrophe indicates that *x', y'* are auxiliary variables and not the final *x, y* coordinates of the space.

The real and imaginary parts of Equation (10) can be separated and the space coordinates can be calculated in terms of *u, v* and *a*:

$$x' = \frac{a}{\pi} \ln\left(\frac{\sin^2(u) + \sinh^2(v)}{\cos^2(u) + \sinh^2(v)} \right) \tag{13}$$

$$y' = \frac{2a}{\pi} \tan^{-1}\left(\frac{\sinh(2v)}{\sin(2u)} \right) - a \tag{14}$$

The 3D space system *(u, v, w)* can be generated by rotating the *x', y'* plane around the *y'* axis. We can find the relationships between the curvilinear space and the Cartesian space:

$$x = \frac{a}{\pi} \ln\left(\frac{\sin^2(u) + \sinh^2(v)}{\cos^2(u) + \sinh^2(v)} \right) Cos(w) \tag{15}$$

$$y = \frac{a}{\pi} \ln\left(\frac{\sin^2(u) + \sinh^2(v)}{\cos^2(u) + \sinh^2(v)} \right) Sin(w) \tag{16}$$

$$z = \frac{2a}{\pi} \tan^{-1}\left(\frac{\sinh(2v)}{\sin(2u)} \right) - a \tag{17}$$

For the sake of simplicity, we will work on the *x-z* plane (*w=0*):

$$\begin{aligned} x &= \frac{a}{\pi} \ln\left(\frac{\sin^2(u) + \sinh^2(v)}{\cos^2(u) + \sinh^2(v)} \right) \\ y &= 0 \\ z &= \frac{2a}{\pi} \tan^{-1}\left(\frac{\sinh(2v)}{\sin(2u)} \right) - a \end{aligned} \tag{18}$$

The *x-z* equations represent two perpendicular sets of parametric curves. The first set (called here the *v-set)* can be generated using *u* as parameter and *v* as a constant. The second set (called the *u-*

set) uses v as parameter, while u is held constant. Figure 2 shows some examples of this family of curves. Notice that if $0 < u < \pi/2$, only the bottom half of the space ($-a < z < 0$) is generated.

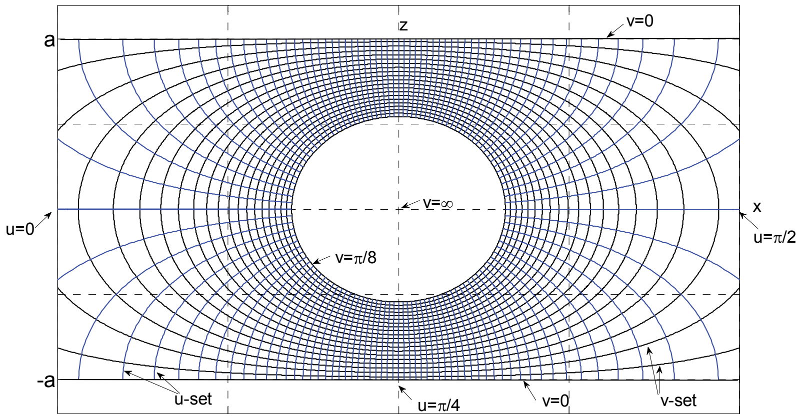

Figure 2 Logarithmic – Tangent curves: *u-set* curves (blue), *v-set* curves (black)

We propose to form the electrodes of the SWO taking a pair of curves belonging to the *v-set* and rotating them around the z axis. The coaxial line section can be connected at the extremities of the curves, at the points where $u=0$, $u=\pi/2$ (the horizontal axis $z=0$).

The parameters of the generated profiles are $v = v_1$ and $v = v_2$ with $0 < u < (\pi/2)$. Note that if a constant difference of potential is applied between v_1 and v_2, the formed potential lines will be conformal to the *v-set* and the electric field stream lines will be conformal to the *u-set*[9]. Note also that, on the x-axis, the stream lines are parallel to the x axis, coinciding with the direction of the stream lines inside the coaxial line (which are radial).

The choice for this coordinate system is justified by the fact that the curves belonging to the *v-set* fulfill the conditions i, ii, and iii, as follows:

Condition i and ii: by simple inspection of Figure 2 it can be concluded that the distance between any pair of curves belonging to *v-set* is minimum on the axis of symmetry (y axis, $u=\pi/4$) and increases as we move away from the axis of symmetry ($u \rightarrow \pi/2, u \rightarrow 0$). This can be demonstrated by calculating the length of an arc *u=constant,* between v_1 and v_2. From Equation (8) this is:

$$l_v(v_2,v_1,u)=\int_{v_1}^{v_2} dl_v = \int_{v_1}^{v_2} \sqrt{g_{22}}\,dv \tag{19}$$

The metric coefficient $g_{22}$is:

$$g_{22}=\left(\frac{4a}{\pi}\right)^2 \frac{1}{\left(Sin[2u]^2+Sinh[2v]^2\right)} \tag{20}$$

Replacing the metric coefficient, Equation (19) becomes:

$$l_v(v_2,v_1,u)=\frac{a4}{\pi}\int_{v_1}^{v_2}\sqrt{\frac{1}{\left(Sin[2u]^2+Sinh[2v]^2\right)}}dv \tag{21}$$

This integral can be expressed as:

$$l_v(v_2,v_1,u)=-\frac{2ia}{\pi}Csc[2u]F[2iv,Csc[2u]^2]\Big|_{v_1}^{v_2} \tag{22}$$

where *F(φ,k)* is the incomplete elliptic integral of the first kind:

$$F(\varphi,k)=\int_0^{\varphi}\frac{d\theta}{\sqrt{1-k^2Sin^2[\theta]}} \tag{23}$$

For a fixed *v,* equation (22) minimizes at $u=\pi/4$, and increases monotonically as *u* moves towards either to 0 or to $\pi/2$, see for example [10] (page 593).We show this in Figure 3, where a contour plot of the function defined by Equation (22) is presented. On this graph,$v_1=0$, a=1 and $0<v<\pi/8$. As it can be seen, the arc length decreases as the variable *u* approaches $\pi/4$.

Condition iii: The full derivative of Equation (9) is:

$$\frac{dZ}{dW}=\frac{2a}{\pi}Csc\left[W\right]Sec\left[W\right] \tag{24}$$

This is continuous for all *W* except for *W=0*.

Note that at the points $u=\pi/2$, $u=0$, the derivative of the v-set is infinite, which corresponds to a vertical line. The coaxial transmission line is connected at this point, assuring the continuity of the derivative of the profile.

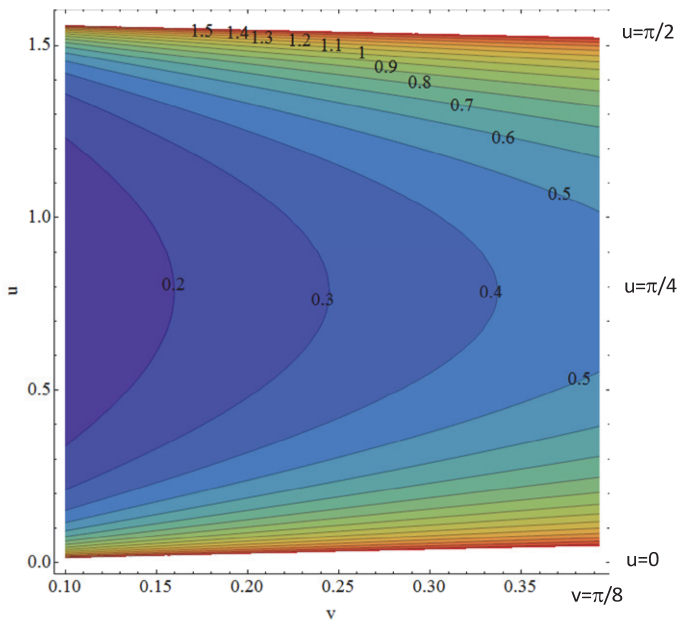

Figure 3 Contour plot of the arc length on the v-axis, as defined by Equation (21); $v_1=0$ and v_2 is varying between 0 and $\pi/8$. Notice that, for a fixed value of v the arc length decreases as u approaches $\pi/4$.

We'll demonstrate in the next section how to integrate the parameters of the design, i.e. conditions iv and v, in the calculation of the profiles.

6. INVERSE FUNCTION OF THE LOG-TAN TRANSFORMATION

At this point it's convenient to express *u* and *v* as a function of *x* and *y*[1].

The basic transformation is:

---

[1]. This was not included in Moon and Spencer's book.

$$Z = \frac{2a}{\pi} Ln\left[Tan[W]\right] - ia \qquad (25)$$

The inverse of which is:

$$W = u + iv = ATan\left[ie^{\frac{Z\pi}{2a}} + i\frac{\pi}{2}\right] \qquad (26)$$

We need to separate the right side of Equation (26) into real and imaginary parts. This can be done by considering the following identity[10] :

$$u + iv = ATan[\alpha + \beta i] = 0.5ATan\left[\frac{2\alpha}{1-\alpha^2-\beta^2}\right] + i\left(\frac{1}{4}Ln\left[\frac{\alpha^2+(\beta+1)^2}{\alpha^2+(\beta-1)^2}\right]\right) \qquad (27)$$

The problem now consists in finding:

$$\alpha = \mathrm{Re}\left[ie^{\frac{Z\pi}{2a}} + i\frac{\pi}{2}\right] \quad ; \quad \beta = \mathrm{Im}\left[ie^{\frac{Z\pi}{2a}} + i\frac{\pi}{2}\right] \qquad (28)$$

Applying the de Moivre's formula to the exponential term and simplifying leads to:

$$ie^{\frac{(x+iy)\pi}{2a}} = i\left(Cos\left[\frac{\pi}{2a}y\right]\left(Cosh\left[\frac{\pi}{2a}x\right] + Sinh\left[\frac{\pi}{2a}x\right]\right) - Sin\left[\frac{\pi}{2a}y\right]\left(Cosh\left[\frac{\pi}{2a}x\right] + Sinh\left[\frac{\pi}{2a}x\right]\right)\right) \qquad (29)$$

From which α and β can be obtained:

$$\begin{aligned} \alpha &= -Sin\left[\frac{\pi}{2a}y\right]\left(Cosh\left[\frac{\pi}{2a}x\right] + Sinh\left[\frac{\pi}{2a}x\right]\right) \\ \beta &= Cos\left[\frac{\pi}{2a}y\right]\left(Cosh\left[\frac{\pi}{2a}x\right] + Sinh\left[\frac{\pi}{2a}x\right]\right) \end{aligned} \qquad (30)$$

Replacing this into Equation (27) permits to find the expressions for *u* and *v* in terms of *x* and *y*:

$$u = Atan\left[\frac{Sin\left[\frac{\pi y}{2a}\right]}{Sinh\left[\frac{\pi x}{2a}\right]}\right] \qquad (31)$$

$$v = \frac{1}{4} Ln\left[\frac{Cosh\left[\frac{\pi x}{2a}\right] + Cos\left[\frac{\pi y}{2a}\right]}{Cosh\left[\frac{\pi x}{2a}\right] - Cos\left[\frac{\pi y}{2a}\right]}\right] \quad (32)$$

7. CALCULATION OF THE SURFACES

The procedure which will be presented in this section aims at finding the values of the parameters v_1, v_2 and a, defining the profiles of the electrodes and satisfying conditions iv and v.

Condition iv: The distance between the curves at $u=\pi/4$ (the axis of symmetry) should be equal to d_{gap}. Using the arc length expression (Equation (21)), this can be calculated as:

$$l_v(v_2, v_1, \pi/4) = d_{gap} = \frac{4a}{\pi}\int_{v_1}^{v_2}\sqrt{\frac{1}{1+Sinh[2v]^2}}dv$$

$$d_{gap} = \frac{4a}{\pi}\left(ArcTan\left[Tanh\left[v_2\right]\right] - ArcTan\left[Tanh\left[v_1\right]\right]\right) \quad (33)$$

Condition v: The RTL is connected to the coaxial line on the x-axis, z=0. On this axis the curvilinear coordinates are ($u=\pi/2$, $v=v_1$) and ($u=\pi/2$, $v=v_2$),while the rectangular coordinates are ($x_1=r_i$, z=0), ($x_2=r_0$, z=0), r_i, r_o being the inner and outer radii of the coaxial transmission line, and x_1, x_2 belong to the v_1 and $v_2$curves, respectively.

Using the arc length expression (Equation (21)), this can be calculated as:

$$l_v(v_2, 0, \pi/2) = x_2 = \frac{4a}{\pi}\int_{0}^{v_2}\sqrt{\frac{1}{Sinh[2v]^2}}dv \quad ; \quad l_v(v_1, 0, \pi/2) = x_1 = \frac{4a}{\pi}\int_{0}^{v_1}\sqrt{\frac{1}{Sinh[2v]^2}}dv \quad (34)$$

$$x_2 = \frac{2a}{\pi} Log\left[Tanh\left[v_2\right]\right] \quad ; \quad x_1 = \frac{2a}{\pi} Log\left[Tanh\left[v_1\right]\right]$$

Inserting Equation (34) into Equation (33) leads to:

$$d_{gap} = \frac{4a}{\pi}\left(ArcTan\left[e^{\frac{\pi x_2}{2a}} \right] - ArcTan\left[e^{\frac{\pi x_1}{2a}} \right] \right)$$

$$Tan\left[\frac{d_{gap}\pi}{4a} \right] = \frac{e^{\frac{\pi x_2}{2a}} - e^{\frac{\pi x_1}{2a}}}{1 + e^{\frac{\pi x_2}{2a}} e^{\frac{\pi x_1}{2a}}} \tag{35}$$

This last equation can be numerically solved, and the value of the constant *a* can be found. Afterwards, the value of the constants v_1 and v_2 can be calculated using Equation (32).

As an example, consider the following case. Let us assume that the inter-electrodic space in a certain SWO is specified as d_{gap}=0.5 mm and the geometrical parameters of the coaxial transmission line are r_o =15 mm and r_i=14 mm (corresponding to an impedance Z_{coax}=4 Ω).

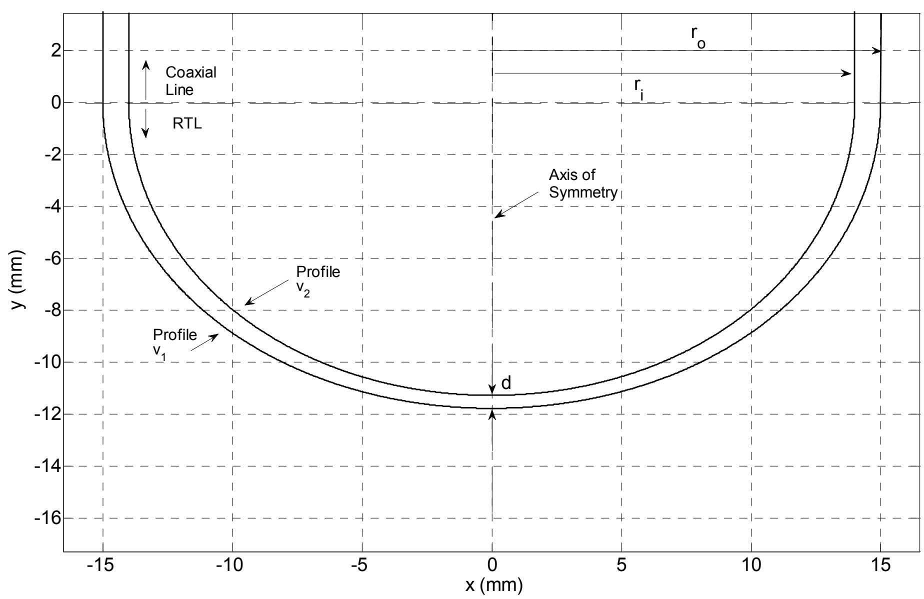

Figure 4 Geometry of the electrodes. Dimensions are in mm

Solving equations (35) and (32), we can calculate the constants defining the profiles, which are given by

$$v_2 = 0.2618, v_1 = 0.2881, a = 17.3e-3$$

Figure 4 shows the resulting geometry.

8. ELECTROSTATIC SIMULATION

The geometry of the considered example was simulated using the electrostatic 2-D axis symmetrical mode in Comsol®. A potential difference of 1V was applied between the electrodes. The boundary conditions of the geometry and the resulting electric field distribution are presented in Figure 5. As it can be seen, the electric field is maximum on the axis of symmetry. The isopotential lines and the electric field streamlines are plotted in Figure 6. As expected, the electric field stream lines are conformal to the *u-set* and the isopotential lines are conformal to the *v-set*. It can be seen that the stream lines are parallel to the *y* axis on the axis of symmetry, and parallel to the *x* axis at the connection point between the coaxial and the RTL.

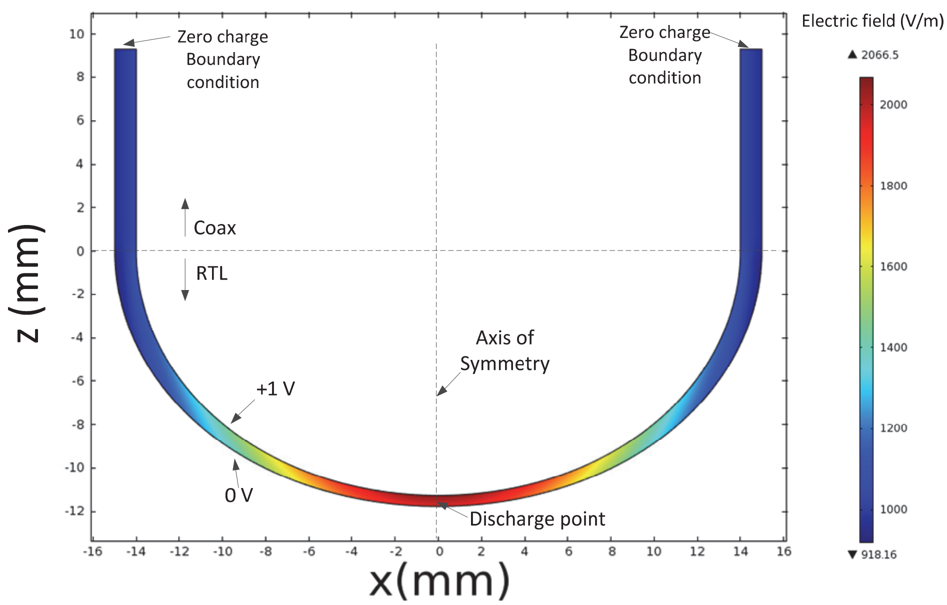

Figure 5. Electric field norm in V/m. Notice that the maximum amplitude occurs at the axis of symmetry

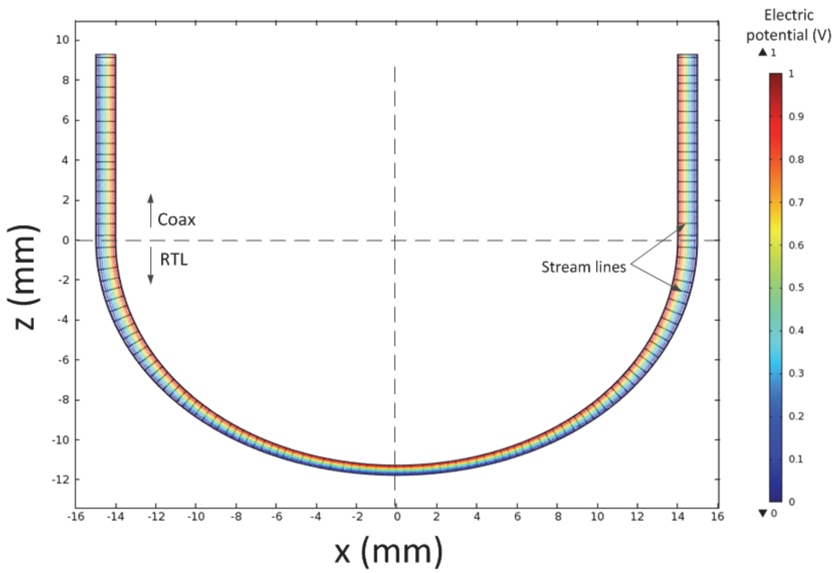

Figure 6. Electric potential in V (colored lines) and electric field stream lines (solid black lines). Notice the progressive change in the direction of the stream lines.

A more detailed plot of the electric field is presented in Figure 7. The electric field was computed along a third curve (v_3) lying in the mid plane between the electrodes. On the axis of symmetry, the distance betweenv_3 and $v_1$is $d_{gap}/2$. In the region where the coaxial line begins, the distance between v_3 and v_1 is $(r_o-r_i)/2$. As it can be seen from this figure, the magnitude of the simulated electric field is maximum on the axis of symmetry and decreases smoothly and monotonically without field enhancements or disturbances up to reaching the coaxial transmission line.

The simulated electric field at the discharge point is E_d=2000 V/m, which corresponds exactly to the electric field in a uniform gap:

$$E_d = \frac{V}{d} = \frac{1(V)}{0.5e-3(m)} = 2000(V/m) \tag{36}$$

The simulated electric field at the midpoint between the conductors of the coaxial is 1000 V/m. This is in agreement with the theoretical value:

$$E_{coax} = \frac{V}{r}\frac{1}{Ln\left(\frac{r_o}{r_i}\right)} = \frac{1(V)}{14.5e-3(m)}\frac{1}{Ln\left(\frac{15e-3(m)}{14e-3(m)}\right)} = 999.6(V/m) \quad (37)$$

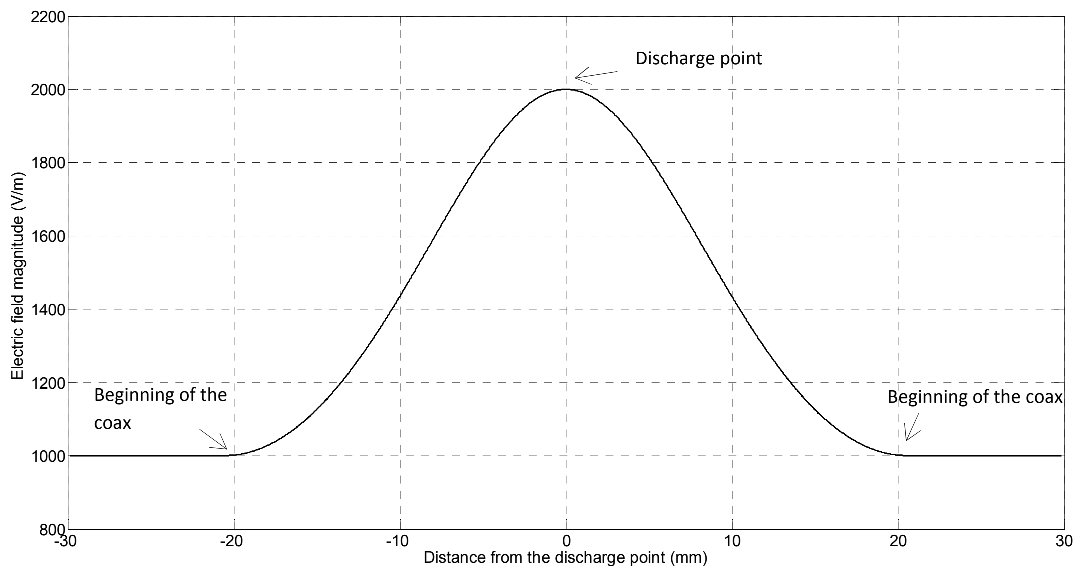

Figure 7Magnitude of the electric field versus distance from the discharge point. The electric field was measured along a *v*-curve equidistant from the electrodes at the discharge point to the coaxial line region. The point 0 on the horizontal axis corresponds to the axis of symmetry. Notice that the electric field decreases smoothly and monotonically.

9. CONCLUSIONS

A new profile for the electrodes forming the radial transmission line of a switched oscillator (SWO) was presented. The profile is formed using a set of conformal curves generated using a specific 2-D transformation called Logarithmic-Tangent (Ln-Tan). We have shown that the proposed profile results in an optimal distribution of the electrostatic field, with peak amplitude occurring on the axis of symmetry of the SWO, and a smooth, monotonic decrease as we move away from the discharge point towards the coaxial transmission line. Moreover, we demonstrated that the proposed profile guarantees a smooth continuity (up to the first space derivative) at the junction of the RTL-coaxial line. The proposed profile was illustrated through an application example for which numerical simulations on the resulting distributions of the electric field and potential obtained using Comsol® were presented and discussed.

Acknowledgements - Financial support from the EPFL-SDC (Swiss Agency for Development and Cooperation) Fund and Armasuisse are acknowledged.

10. REFERENCES

[1] C. E. Baum, "Switched Oscillators," *Circuit and Electromagnetic System Design Notes,* 200.

[2] P. Moon and D. E. Spencer, *Field Theory Handbook: Including Coordinate Systems, Differential Equations and Their Solutions* 2ed.: Springer-Verlag, 1971.

[3] W. Rogowski, "Die elektrische Festigkeit am Rande des Plattenkondensators," *Archiv f?r Electrotechnik,* vol. 12, pp. -, 1923.

[4] G. J. Ernst, "Uniform-field electrodes with minimum width," *Optics Communications,* vol. 49, pp. -, 1984.

[5] F. M. Bruce, "Calibration of uniform-field sparkgaps for high-voltage measurement at power frequencies," *Journal of IEE, pt.II,* vol. 94, pp. -, 1947.

[6] D. V. Giri*, et al.*, "Switched Oscillators and Their Integration Into Helical Antennas," *Plasma Science, IEEE Transactions on,* vol. 38, pp. 1411-1426, 2010.

[7] M. Armanious*, et al.*, "Electrostatic field management and electrodynamic modeling of switched quarter-wave oscillators," *Dielectrics and Electrical Insulation, IEEE Transactions on,* vol. 18, pp. 1054-1065, 2011.

[8] P. Moon and D. E. Spencer, "Cylindrical and Rotational Coordinate Systems," *Journal of Franklin Institute,* vol. 52, p. 327, 1951.

[9] F. Gardiol, *Électromagnétisme*, 2 ed. vol. 3. Lausanne, Switzerland: Éditions Georgi, 1979.

[10] M. Abramowitz and I. Stegun, *Handbook of mathematical functions*: National Bureau of Standards, 1972.